

# Reflection of Pulse Waves and Resonance Characteristics of Arterial Beds

N. N. Kizilova

Received August 29, 2002

**Abstract** — The problem of axisymmetric wave flow of a viscous incompressible fluid in a system consisting of a long thin deformable tube and a terminal element that determines the conditions of wave reflection at the tube end is analyzed. An expression for the input admittance of the system is obtained and the dependence of the admittance on the system parameters is investigated. The resonant frequencies at which the admittance amplitude has extrema are found and it is shown that at these frequencies the admittance variations with variation of the terminal-element parameters are maximal. The dependence of the resonant frequency on the tube length is investigated. Possible applications of the results obtained to the hydromechanical interpretation of a novel method of pulse diagnostics are discussed.

**Keywords:** waves in elastic tubes, input admittance, pulse diagnostics, spectral analysis.

The characteristics of the propagation and reflection of pressure waves in fluid-filled dilatable tubes have been studied in hydromechanics, in particular, in connection with the opportunities for pulse diagnostics. Following the tradition of oriental medicine, the state of 10–12 internal organs can be detected from the pulse characteristics of the radial artery in the wrist. One novel approach is based on the presence of resonant harmonics in the vascular systems of the internal organs, different for different organs. The amplitudes of these harmonics change considerably in pathological states of the organ, whereas the amplitudes of the other harmonics change only slightly [1–6]. The novel method makes it possible to diagnose on the basis of the pressure spectrum characteristics recorded by a sphygmomanometer in an arbitrary peripheral artery convenient for measurement. The presence of resonant frequencies and the mechanisms of variation of the corresponding amplitudes are still insufficiently explored in hydrodynamic terms, whereas the method itself is being used in clinical practice [3, 5, 6].

Below, on the basis of a model of incompressible viscous wave flow in a deformable tube with a terminal resistance, we investigate the resonance characteristics of the system and the effect of its parameters on the characteristics of the reflected wave.

## 1. RESONANCE CHARACTERISTICS OF ARTERIAL BEDS

Experimental pulse investigations have shown that in states classified in oriental medicine as excess (deficiency) syndromes the amplitudes of the corresponding resonant pressure harmonics turn out to be 30–40 % higher (lower) than their normal values, depending on the intensity of the syndrome [1–4]. In clinical studies, the resonant harmonics have been found for several internal organs [3, 4] and the effect of therapeutic treatment on the pulse spectrum characteristics of the human radial artery has been studied [5, 6]. The presence of resonant harmonics has been confirmed by *in vivo* measurements using a micromanometer [2, 4] and on a model of the blood circulation system consisting of a compliant tube and a system of elastic chambers [1, 7].

In blood circulation hydromechanics, for describing the characteristics of the arterial bed, the input admittance  $Y_{in}$  defined as the ratio of the flow-rate amplitude  $Q$  to the pressure amplitude  $P$  at the supplying-artery inlet,  $Y_{in} = Q/P$ , is used. The resonance characteristics of the vascular beds of organs may have their

origin in the laws of wave reflection in an arterial tree with a definite geometry. The bed input admittance depends on the frequency  $\omega$  of the harmonic and may be either less or greater than the admittance of the supplying artery [8–10]. Experimental *in vivo* measurements have shown that the resonant harmonics correspond to extrema of the admittance  $Y_{in}(\omega)$  [4]. Since the internal organs are incorporated in the general blood circulation system, a pathological change in the organ's vascular-bed conductance must change the parameters of the pulse wave it reflects and, hence, the pressure spectrum characteristics in the peripheral artery used for diagnostic purposes.

At the inlet to the arterial bed of an organ, the pulse wave parameters are determined by the characteristics of the heart and aorta and the reflection conditions in the aorta — internal organs system. In the problem considered, we will assume these parameters to be given and analyze the wave reflection characteristics in the arterial bed of the organ and the spectral characteristics of the input admittance.

## 2. WAVE REFLECTION IN THE TUBE — TERMINAL RESISTANCE SYSTEM

As a simple model of the arterial bed of an organ, we will consider a long thin elastic circular tube with the undisturbed cross-section area  $S_0$  and length  $L$ , where  $\sqrt{S_0}/L \ll 1$ , connected in series with a terminal element with the admittance  $Y_t$ . We will assume the system considered to be incorporated as a separate element in a general model of the arterial bed in such a way that at the tube inlet the pressure  $p_{in}(t) = Pe^{i\omega t}$ , where  $\omega = 2\pi f$  and  $f$  is the wave frequency, is given and in the tube inlet cross-section the pressure and the volume flow-rate are recorded.

We will consider an axisymmetric flow of a homogeneous incompressible viscous fluid with the density  $\rho$  and, on the assumption that the tube compliance  $\lambda$  is small, use the equations of motion in the quasi-one-dimensional approximation [11–13]:

$$\frac{\partial S}{\partial t} + \frac{\partial}{\partial x}(SU) = 0 \quad (2.1)$$

$$\frac{\partial U}{\partial t} + U \left( \frac{\partial U}{\partial x} + \frac{8\pi\nu}{S} \right) + \frac{1}{\rho} \frac{\partial p}{\partial x} = 0 \quad (2.2)$$

$$s = \lambda(p - p_0) + S_0 \quad (2.3)$$

with the corresponding inlet conditions and pressure and flow-rate continuity conditions at the end of the tube:

$$x = 0: \quad p = p_{in}(t); \quad x = L; \quad p = Q_t(t)/Y_t, \quad Q = Q_t(t) \quad (2.4)$$

where  $x$  is the longitudinal coordinate measured from the tube inlet cross-section,  $S(t, x)$  is the cross-section area,  $U(t, x)$  is the longitudinal velocity averaged over the cross-section,  $p(t, x)$  is the pressure,  $p_0$  and  $S_0$  are the undisturbed pressure and cross-section area,  $\nu$  is the kinematic viscosity of the fluid,  $Q = US$ , and  $Q_t(t)$  is the flow-rate in the inlet cross-section of the terminal element.

The system (2.1)–(2.3) linearized about the rest state describes the propagation of small perturbations up- and downstream (forward and backward waves) at the speed

$$c = c_0 \sqrt{\frac{2}{\sqrt{\xi^2 + 1} + 1}}, \quad \xi = \frac{8\pi\nu}{\omega S_0}, \quad c_0 = \sqrt{\frac{S_0}{\rho\lambda}}$$

where  $c_0$  is the perturbation propagation velocity in an ideal fluid. We will seek the solution of (2.1)–(2.4) in the form:

$$p(t, x) = p_0 + p^* e^{i\omega t} e^{-\gamma x}, \quad U(t, x) = U^* e^{i\omega t} e^{-\gamma x} \quad (2.5)$$

Substituting (2.5) in the linearized equations (2.1)–(2.2), we obtain:

$$\gamma = \frac{\omega}{c_0} \sqrt{i\xi - 1}, \quad \alpha = \text{Re}(\gamma) = \frac{\omega}{c_0} \sqrt{\frac{1 + \xi^2 - 1}{2}}$$

Here,  $\alpha$  determines the wave damping and  $\text{Im}(\gamma) = \omega/c = k$  is the wave number. For small pressure and flow-rate perturbations, denoting the amplitudes of the forward and backward waves by  $p_f$  and  $p_b$ , respectively, we obtain the solution in the form of a superposition of the following functions (here and in what follows, the superscript corresponding to the disturbed variables is omitted):

$$\begin{aligned} p(t, x) &= p_f e^{i\omega t} (e^{-\gamma x} + \Gamma e^{\gamma(x-2L)}), & \Gamma &= \frac{p_b}{p_f} \\ Q(t, x) &= Y p_f e^{i\omega t} (e^{-\gamma x} - \Gamma e^{\gamma(x-2L)}), & Y &= \frac{S_0}{\rho c_0} \end{aligned} \quad (2.6)$$

where  $Y$  is the characteristic admittance of the tube (admittance in the absence of reflected waves [11]) and  $\Gamma$  is the reflection coefficient at the junction of the tube and the terminal element. For  $x = L$ , from (2.6), we have:

$$p(t, L) = p_f e^{i\omega t - \gamma L} (1 + \Gamma), \quad Q(t, L) = Y p_f e^{i\omega t - \gamma L} (1 - \Gamma) \quad (2.7)$$

From (2.7), using (2.4), we obtain  $\Gamma = (Y - Y_t)/(Y + Y_t)$ . Now, from (2.6), introducing the input admittance of the system  $Y_{in} = Q(t, 0)/p(t, 0)$ , we have:

$$Y_{in} = Y \frac{Z + i \tan(kL)}{1 + iZ \tan(kL)}, \quad Z = \frac{Y \tanh(\alpha L) + Y_t}{Y + Y_t \tanh(\alpha L)} \quad (2.8)$$

The quantity  $Y_{in}$  determines the parameters of the wave reflected by the system. If  $kL \ll 1$  or  $kL = \pi n$ , where  $n \in N$ , it follows from (2.8) that  $Y_{in} = YZ$ . As  $\alpha L \rightarrow 0$ , from (2.8), we obtain  $Y_{in} = Y_t$ . Generally,  $Y_t = Y_1 + iY_2$ , where  $Y_1$  is the real part of the admittance of the terminal element and the quantity  $Y_2$  is related with its compliance and determines the change in the wave phase after reflection in the cross-section  $x = L$  [11]. If  $Y_2 = 0$ ,  $\text{Im}(\Gamma) = 0$  and the reflected and transmitted waves are in phase. For  $\text{Re}(\Gamma) = 1$  reflection from the closed ( $Y_t = 0$ ) end of the tube takes place, whereas for  $\text{Re}(\Gamma) = 0$  there is no reflected wave. In the latter case, the input and characteristic admittances of the tube coincide:  $Y_{in} = Y = Y_t$ . From (2.8), substituting the input admittance in the form  $Y_{in} = Y_0 e^{i\psi}$ , we obtain the following relations for the parameters  $y_0 = Y_0/Y$  and  $\psi$ :

$$y_0 = \left( \frac{Z_1^2 + Z_2^2 + 2Z_2\varphi + \varphi^2}{1 + 2Z_2\varphi + (Z_1^2 + Z_2^2)\varphi^2} \right)^{1/2} \quad (2.9)$$

$$\psi = \arctan \left( \frac{Z_2(1 - \varphi^2) + (1 - Z_1^2 - Z_2^2)\varphi}{Z_1(1 + \varphi^2)} \right) \quad (2.10)$$

$$\begin{aligned} Z_1 &= \frac{(1 + y_1^2 + y_2^2)\tau + y_1(1 + \tau^2)}{1 + 2y_1\tau + (y_1^2 + y_2^2)\tau^2}, & Z_2 &= \frac{y_2(1 - \tau^2)}{1 + 2y_1\tau + (y_1^2 + y_2^2)\tau^2} \\ \varphi &= \tan(kL), & \tau &= \tanh(\alpha L), & y_1 &= Y_1/Y, & y_2 &= Y_2/Y \end{aligned}$$

### 3. ANALYSIS OF THE SYSTEM INPUT ADMITTANCE CHARACTERISTICS

For fixed non-zero  $y_1$  and  $y_2$ , the functions  $y_0(\varphi, \tau)$  and  $\psi(\varphi, \tau)$  are continuous and bounded and have the limiting values

$$\begin{aligned} y_0(0, 0) &= (y_1^2 + y_2^2)^{1/2}, & y_0(\pm\infty, \pm\infty) &= (y_1^2 + y_2^2)^{-1/2} \\ \psi(0, 0) &= \psi(\pm\infty, \pm\infty) &= \arctan(y_2/y_1) \end{aligned}$$

From (2.9), it follows that the input admittance of the system considered is greater than the characteristic admittance of the tube ( $y_0 > 1$ ) if the conditions  $Y_1^2 + Y_2^2 > Y^2$ ,  $|\varphi| < 1$  or  $Y_1^2 + Y_2^2 < Y^2$ ,  $|\varphi| > 1$  are satisfied. Otherwise,  $y_0 < 1$ . If  $Y$ ,  $Y_1$ , and  $Y_2$  are linked by a definite relation, the input admittance of

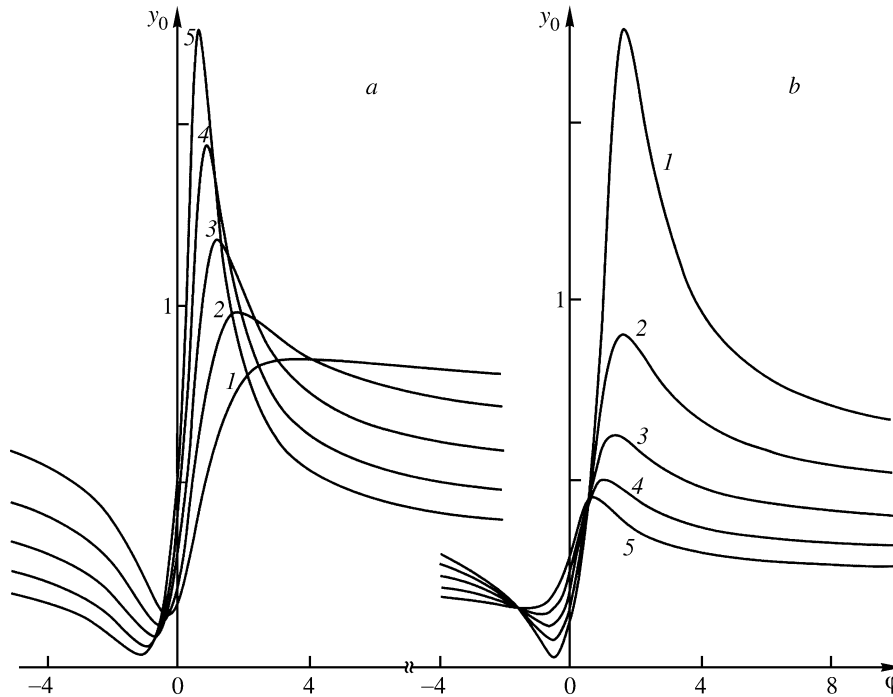


Fig. 1. Families of curves  $y_0(\varphi)$  for  $y_1 = 0.5$ ;  $y_2 = 0.2, 0.4, 0.6, 0.8, 1$  (a) and  $y_1 = 0.2, 0.4, 0.6, 0.8, 1$ ;  $y_2 = 0.5$  (b)

the system  $Y_{in}$  is, for certain harmonics, greater or less than the characteristic admittance of the tube. The frequencies of the corresponding harmonics can then be found from the conditions  $|\varphi| > 1$  and  $|\varphi| < 1$ . In a particular case, for  $\xi = 0$ ,  $Y_2 = 0$  and  $kL = \pi/2$ , and for  $Y_1 = 0$  these characteristics were analyzed in [11]. As  $\tau \rightarrow 0$  in (2.9)–(2.10), we have  $Z_1 = y_1$  and  $Z_2 = y_2$ .

If the conditions  $kL \ll 1$  or  $kL \sim \pi$  are satisfied, then (2.9)–(2.10) degenerate into the relations  $y_0 = (Z_1^2 + Z_2^2)^{1/2}$  and  $\psi = \arctan(Z_2/Z_1)$ . The tube then transmits the incident wave with the phase unaltered (if  $kL \sim 0$ ) or changed by  $\pi$  (if  $kL \sim \pi$ ) and its length does not affect the parameters of the reflected wave.

For  $y_1 = 1$  and  $y_2 = 0$ , if the admittances of the tube and the terminal element are matched and there is no reflected wave,  $Z_1 = 1$ ,  $Z_2 = 0$  and  $y_0 = 1$ ,  $\psi = 0$ . Correspondingly, for  $Y_t = 0$  (reflection from the closed end of the tube), from (2.9)–(2.10) we obtain the relations:

$$y_0 = \left( \frac{\tau^2 + \varphi^2}{1 + \tau^2 \varphi^2} \right)^{1/2} \quad \tan(\psi) = \frac{(1 - \tau^2)\varphi}{(1 + \varphi^2)\tau}$$

Since  $\tau < 1$ , with increase in  $\alpha L$  the admittance amplitude  $y_0$  increases if  $0 < |\varphi| < 1$  and decreases if  $|\varphi| > 1$ . Correspondingly, with increase in  $\alpha L$ ,  $\psi$  monotonically decreases and  $\psi > 0$  for  $\varphi > 0$ . In the limiting case  $\xi = 0$ , from (2.9)–(2.10) we find, as in [11],  $y_0 = \varphi$  and  $\psi = \pm\pi/2$ .

We will now investigate the resonant, in the sense of [1–6],  $\omega$  values at which  $y_0(\omega)$  reaches an extremum. The requirement  $(y_0)'_{\omega} = 0$  leads to a transcendental equation for  $\omega$  which can be solved numerically for specified values of the parameters  $y_{1,2}$ ,  $L$ ,  $c_0$ , and  $\xi$ .

We will consider the case  $\xi < 1$ . Since  $\xi = \xi_0/f$  and  $\xi_0 = 4\nu/S_0$ , this case corresponds to high-frequency harmonics of the pulse wave and, if for a certain harmonic with frequency  $f_0$  the condition  $\xi_0 < 1$  is satisfied, this condition must also be satisfied for all  $f > f_0$ . Certain estimates for the domain of applicability of this case will be presented in Sect. 4. Expanding  $\alpha(\xi)$  in series, we obtain:

$$\tau = \tanh \left( \frac{\pi L \xi_0}{c_0} \left( 1 - \frac{\xi^2}{4} + O(\xi^4) \right) \right)$$

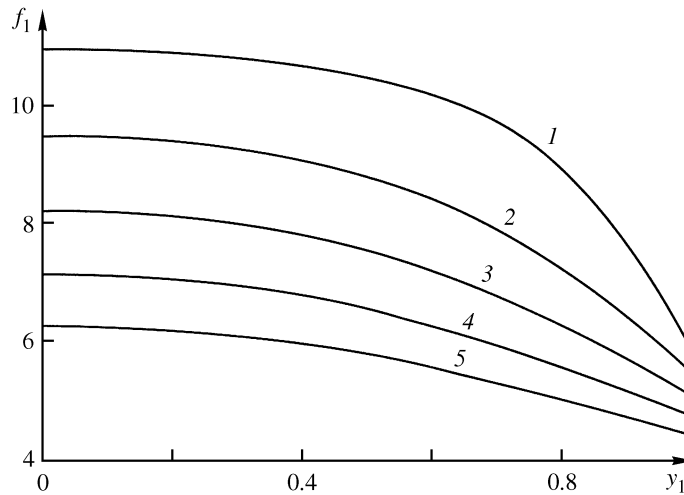


Fig. 2. Families of curves  $f_1(y_1)$ . Curves 1–5 correspond to  $y_2 = 0.2, 0.4, 0.6, 0.8, 1$

Neglecting terms of the order of  $\xi^2$ , we will assume  $\tau \approx \tanh(\pi L \xi_0 / c_0) \equiv \tau_0$ . We will now consider the functions  $y_0(\varphi, \tau_0)$  and  $\psi(\varphi, \tau_0)$ . The condition  $(y_0)'_{\varphi} = 0$  gives the quadratic equation for  $\varphi$

$$Z_2(\tau_0)(\varphi^2 - 1) + (Z_1^2(\tau_0) + Z_2^2(\tau_0) - 1)\varphi = 0$$

with the roots

$$\varphi_{1,2} = \frac{1 - Z_1^2(\tau_0) - Z_2^2(\tau_0) \pm \sqrt{\Theta}}{2Z_2(\tau_0)} \quad (3.1)$$

$$\Theta = (Z_1^2(\tau_0) + Z_2^2(\tau_0))^2 + 1 - 2Z_1^2(\tau_0) + 2Z_2^2(\tau_0)$$

Here,  $\varphi_1 > 0$  determines the maximum and  $\varphi_2 < 0$  the minimum of the function  $y_0(\varphi, \tau_0)$ . In Fig. 1, as an illustration, the families of curves  $y_0(\varphi, \tau_0)$  are presented for several  $y_{1,2}$  values. For a fixed  $y_1$ , the maximum value of  $y_0$  increases and its minimum decreases with increase in  $y_2$ . For a fixed  $y_2$  the same regularities can be observed with decrease in  $y_1$ . For a purely resistive terminal element ( $y_2 = 0$ ), in the case of an ideal fluid ( $\xi_0 = 1$ ), these features were studied in [11].

The functions  $y_0(\omega)$  and  $\psi(\omega)$  are periodic; therefore, in both the amplitude and phase spectra, local maxima and minima corresponding to the resonant frequencies must alternate. From the condition  $\tan(\omega L / c(\omega)) = \varphi_{1,2}$  we can find the frequencies  $\omega_{1,2}$  resonant for a tube of length  $L$  in the sense that the amplitudes of the corresponding harmonics are maximal (minimal) among the amplitudes of all harmonics of the reflected wave. Solving this condition for  $\omega$  yields:

$$\omega_{1,2} = \frac{2c_0^2 \arctan^2(\varphi_{1,2})}{L \sqrt{\xi_0^2 L^2 + 4c_0^2 \arctan^2(\varphi_{1,2})}}$$

In Fig. 2, the families of curves  $f_1(y_1) = \omega_1 / (2\pi)$  are depicted for several fixed  $y_2$  values and  $L = 10$  cm. The corresponding dependences  $f_2(y_1) = \omega_2 / (2\pi)$  can be obtained from those presented in Fig. 2 by means of the parallel translation  $k_2 = k_1 + \arctan(z_2(\tau_0)\sqrt{\Theta} / (z_1^2(\tau_0) + z_2^2(\tau_0))) / L$ . The dependences  $f_{1,2}(y_2)$  at fixed  $y_1$  are of similar form. Thus, if  $0 \leq y_{1,2} \leq 1$ , the resonant frequencies  $f_{1,2}$  vary within a single harmonic (in Fig. 2, for  $f_1 = 1$  Hz, this harmonic is  $n = 4$ ).

The level lines of the functions  $y_0(y_2, f)$  and  $\psi(y_2, f)$  at fixed  $y_1$  are presented in Fig. 3. The regions where the lines become denser correspond to maxima of  $y_0$  (Fig. 3a) and zeros of  $\psi$  (Fig. 3b), whereas the rarefaction zones correspond to minima of  $y_0$  (Fig. 3a) and extrema of  $\psi$  (Fig. 3b). From Fig. 3a, it

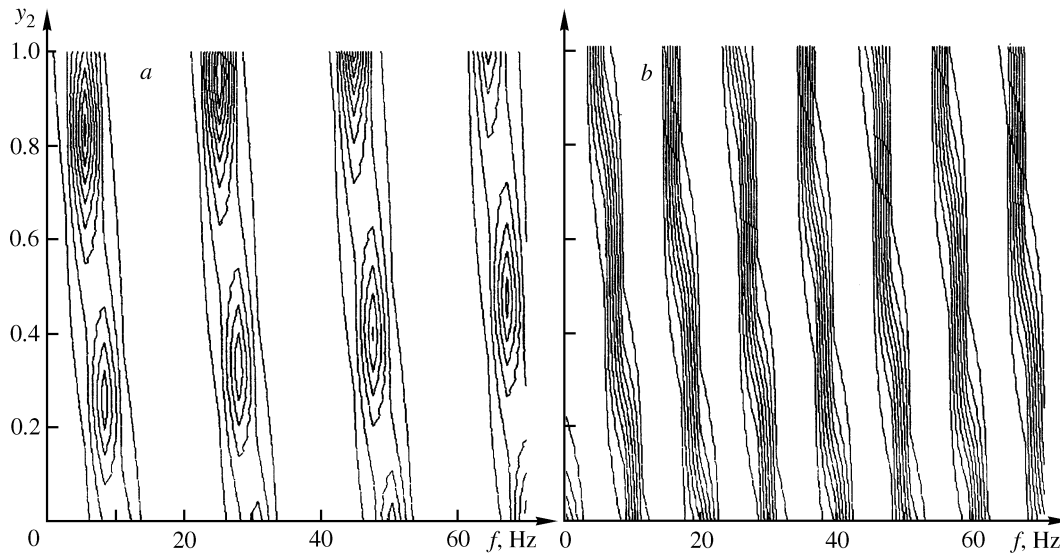


Fig. 3. Level lines of the functions  $y_0(y_2, f)$  (a) and  $\psi(y_2, f)$  (b) for  $y_1 = 0.5$ ,  $c_0 = 10^3$  cm/s, and  $L = 20$  cm

can be seen that the regions of  $y_0$  maxima correspond to narrow ranges in the neighborhood of the resonant frequencies. The variation of the resonant frequencies with variation in  $y_1$  and  $y_2$  can, in general, be estimated by finding the frequency range  $[f - f_1, f + f_1]$  for which the variations of  $y_0(f)$  do not exceed  $\beta y_0(f_1)$ , where  $0 < \beta < 1$ . The boundary frequencies of this interval can be found from the condition  $y_0(\varphi(f)) = \beta y_0(\varphi(f_1))$  which, with account for (2.10), leads to the quadratic equation for  $\varphi(f)$

$$(1 - (y_1^2 + y_2^2)\beta_0^2)\varphi^2(f) + 2y_2(1 + \beta_0^2)\varphi(f) + y_1^2 + y_2^2 - \beta_0^2 = 0$$

$$\beta_0 = \beta y_0(\varphi(f_1))$$

Finding the positive root  $\varphi_+$ , we obtain a general estimate for the resonant-frequency variation:  $f \in [f_1 - \delta, f_1 + \delta]$ , where  $\delta = \arctan(\varphi_+)c/(2\pi L f_1) - 1$ .

#### 4. NUMERICAL CALCULATIONS AND DISCUSSION

If  $L$  is the length of the artery supplying an organ and  $Y_t$  the admittance of the downstream vascular bed, then taking into account the differences in body sizes and the individual characteristics of the bed,  $L$  may vary over a wide range:  $2 \leq L \leq 20$  cm [14, 15]. For arteries of the elastic and muscular types, normal and with a pathological or age-related decrease in the vascular-wall compliance,  $500 \leq c_0 \leq 2500$  cm/s. For the other parameters of the model, we will assume the ranges  $3.8 \cdot 10^{-2} < \nu < 5.7 \cdot 10^{-2}$  cm<sup>2</sup>/s and  $0.2 < r < 0.5$  cm [11, 13], where  $r = \sqrt{S_0/\pi}$ . Estimating, we obtain the inequality  $\xi_0 \leq 0.807$  and, therefore, for  $f_0 = 1\text{--}1.25$  Hz, which corresponds to the human pulse at rest, the approximation  $\xi < 1$  considered above holds for all harmonics. The condition  $\xi < 1$  is not satisfied for vessels of sufficiently small radius but in this case, due to the Fareus-Lindqvist effect,  $\mu = \mu(r)$  and the model considered must be supplemented and analyzed separately.

For variation of the parameters on the range  $0 \leq y_{1,2} \leq 1$ ,  $y_0(t_2)/y_0(t_1) \leq \beta \leq 1$ , a numerical analysis of the dependence  $\delta(y_1, y_2, c, L, \beta)$  has shown that  $\delta \in [0, 3.3]\%$ . Thus, on a wide range of the model parameters, the corresponding variations in the resonant frequency are concentrated within a narrow neighborhood of a single harmonic. Applied to the analysis of the pulse spectrum in a peripheral artery, this means that all pathological changes in the conductance of the arterial bed lead to changes in the system admittance amplitude in the neighborhood of a resonant harmonic, which is consistent with the results of [1–6].

In Fig. 4, as an illustration, the dependences of the amplitude  $y_0(n)$  and the phase  $\psi(n)$  on the harmonic number  $n$  are presented for  $n = 1\text{--}10$ . The range  $n = 1\text{--}10$  can be analyzed spectrally when the pulse

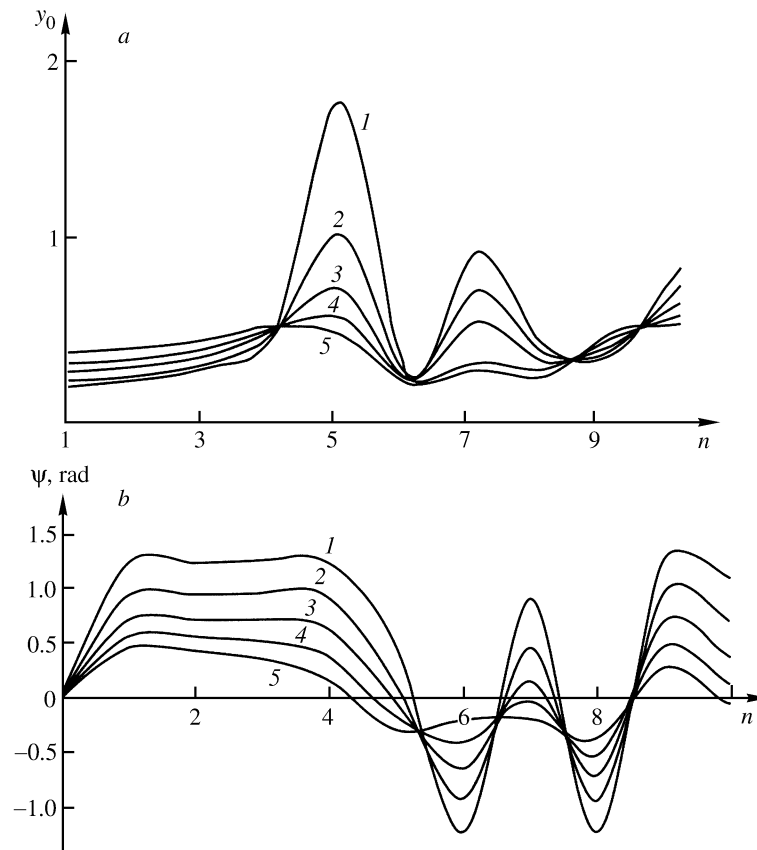


Fig. 4. Dependences  $y_0(n)$  (a) and  $\psi(n)$  (b) on the harmonic number  $n$  for  $n = 1-10$ ,  $L = 10$  cm,  $c_0 = 1500$  cm/s,  $y_2 = 1$ , and  $\nu_0 = 1$  Hz. Curves 1–5 correspond to  $y_1 = 0.2, 0.4, 0.6, 0.8, 1$

of the radial artery is recorded using a cuff sensor [1–6]. In the case considered, maximum admittance amplitude variations can be observed for the harmonics with  $n = 4$  and  $7$ , the corresponding phases being equal to zero. When analyzing a discrete spectrum, small variations in the resonant-harmonic amplitude in the neighborhood of the corresponding Fourier-component may, for small  $y_{1,2}$  deviations, be imperceptible, whereas the phase variations near the resonant harmonic are more discernible, being associated with a change in its sign, and therefore preferable for pulse spectrum analysis [4–6].

For the chosen parameter range, the range of  $kL = 2\pi Lf/c$  can be estimated by the inequality  $0.01f \leq kL \leq 0.2f$ . Hence, in accordance with (2.8), for the low-frequency range ( $n = 1-2$  for  $f_0 = 1$  Hz) we have  $Y_{in} \sim Y_t$ . If  $kL \in [\pi(1/2 + m); \pi(1 + m)]$ , then  $t < 0$  and if  $kL \in [\pi m; \pi(1/2 + m)]$ , then  $t > 0$  (Fig. 1). Hence, for each  $L$ , there exist several frequencies at which  $y_0$  reaches an extremum; in this case the  $y_0$  variations, when  $y_{1,2}$  is varied, are maximal and the phases of the reflected and incident waves coincide. On each of the segments corresponding to  $m = 0, 1 \dots$  there exists a single pair of  $t_{1,2}$  values which determines the resonant frequencies  $\omega$  from the equation

$$2\pi L\omega = \arctan(t_{1,2}(y_1, y_2))c(\omega) \quad (4.1)$$

The results of the  $L(\omega)$  calculations are presented in Fig. 5. All the dependences have the form  $\omega \sim L^{-2}$ , which corresponds to the results of experiments [1, 7].

In accordance with clinical data [2–6], the fundamental resonant frequencies of the vasculatures of human internal organs correspond to successive spectrum harmonics in the following order: liver ( $n = 1$ ), kidneys (2), spleen (3), lungs (4), stomach (5), gall (6) and urinary (7) bladders. The constant pressure component ( $n = 0$ ) is associated with the heart, after which the state of all the internal organs traditionally considered

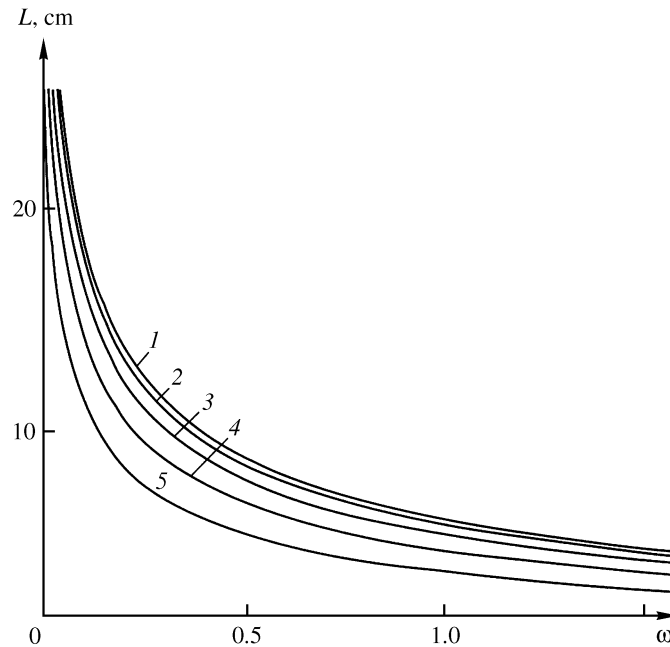


Fig. 5. Dependence  $L(\omega)$ . Curves 1–5 correspond to  $y_1 = 0.2, 0.4, 0.6, 0.8, 1$ ;  $y_2 = 0.5$

in oriental medicine can be diagnosed from the amplitude variation of the corresponding harmonic. This approach is empirical and needs additional detailed estimates based on morphometric data for the beds of the various organs. A monotonic increase in the frequency of the fundamental harmonic  $f_0$  in the above-mentioned sequence of organs means, if the dependence  $f(L)$  holds, that the  $L$  value of the corresponding organ should monotonically decrease in the direction liver  $\rightarrow$  urinary bladder. In morphometric studies of the vascular beds of organs, such regularities have not yet been observed. Although they could occur, for example, in the case of geometric or allometric similarity between the beds of different organs, nevertheless, due to individual variations in the bed parameters [15], a strict order in  $L$  for the different internal organs seems to be an idealization.

Using (2.9), (2.10), and (3.1), we will estimate the  $L$  effect on the resonant parameters of the model. In accordance with the approach adopted in [2–6], the resonant harmonic for  $m = 0$  is assumed to be fundamental (I) and the next one, for  $m = 1$ , additional (II). The calculation results are presented in Fig. 6. The fundamental (I) harmonics are represented by curves and the additional (II) harmonics by symbols. The variations in  $y_{1,2} \in [0, 1]$  lead to changes in amplitude for the same fundamental (I) and additional (II) harmonics. With increasing  $L$  the fundamental harmonic decreases, remaining constant on intervals of length  $\delta L \sim 3\text{--}8$  cm. However, the range of individual variations in supplying-artery length may be considerably wider. For example, for the human lung tree,  $L = 10\text{--}25$  cm [14], which gives a three-harmonic scatter for different  $c_0$  values. The additional harmonics always lie within the high-frequency region of the spectrum, which is consistent with the data presented in [2–6].

An increase in  $c_0$  from 500 to 2000 cm/s leads to a shift of the corresponding resonant frequencies into the high-frequency region by one or two harmonics. The changes in  $c_0$  may be associated with a decrease in the vascular-wall compliance as a result of the development of atherosclerosis, hypertension, or other processes with large characteristic times. Significant short-duration changes in the resonance pattern are a result of complicated blood-flow redistributions, for example, after food intake [16].

**Summary.** The model of the vascular bed as a tube with a terminal element demonstrates a behavior selective with respect to different harmonics of the incident wave. For certain harmonics, the bed admittance is maximal and any changes in the characteristics of the terminal element lead to considerable changes in the amplitude of this harmonic which can be assumed to be resonant. Since the bed of a specific organ



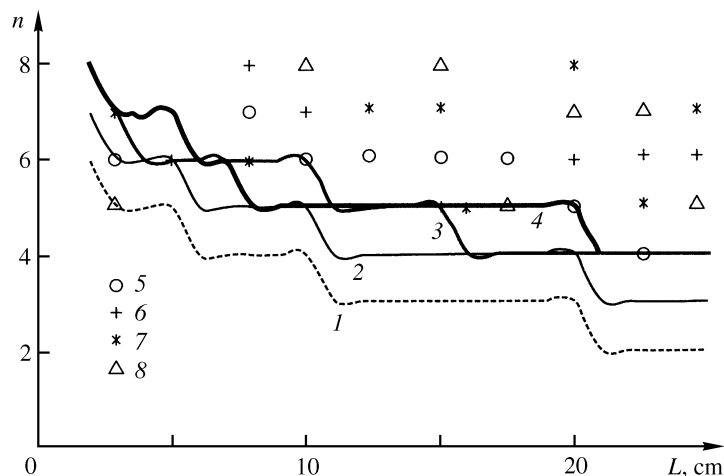


Fig. 6. Number of the resonant harmonic  $n$  vs. tube length  $L$ . The fundamental harmonics for  $c_0 = 500, 1000, 1500$ , and  $2000$  cm/s are numbered 1–4. The corresponding additional harmonics are numbered 5–8

is incorporated in the general blood circulation system, this means that the contribution of the resonant-harmonic amplitude to the reflected wave must be minimal. In the vascular system, waves are reflected at each branching including the offshoots of the arteries supplying all the internal organs. As a result of the difference in the resonant harmonics of the arterial systems for different organs, changes in the state of a single organ can be detected in the pulse spectrum of an arbitrary peripheral artery convenient for measurement, which makes it possible to apply pulse diagnostics using the method proposed in [1–6].

Conclusions and recommendations important for clinical practice can be based on the model presented if data on the quantitative changes in the real and imaginary parts of the terminal-bed admittance in different pathologies are available. We still do not clearly understand the problem of diagnosing combined pathologies when the fundamental resonant harmonic for one organ is the additional resonant harmonic for another and the corresponding changes associated with the pathologies of the two organs are differently directed.

The author is deeply grateful to S. A. Regirer for his interest in this study and stimulating discussions.

## REFERENCES

1. Y. Y. Wang, S. L. Chang, Y. E. Wu, T. L. Hsu, and W. K. Wang, "Resonance. The missing phenomenon in hemodynamics," *Circ. Res.*, **69**, No. 1, 246–249 (1991).
2. G. L. Yu, Y. L. Wang, and W. K. Wang, "Resonance in the kidney system of rats," *Amer. J. Physiol.*, **267**, No. 4, Pt 2, H1544–1548 (1994).
3. W. A. Lu, C. H. Cheng, Y. Y. Lin Wang, and W. K. Wang, "Pulse spectrum analysis of hospital patients with possible liver problems," *Amer. J. Clin. Med.*, **24**, No. 3–4, 315–320 (1996).
4. S. T. Young, W. K. Wang, L. S. Chang, and T. S. Kuo, "The filter properties of the arterial beds of organs in rats," *Acta Physiol. Scand.*, **145**, No. 4, 401–406 (1992).
5. W. K. Wang, J. G. Bau, T. L. Hsu, and Y. Y. Wang, "Influence of spleen meridian herbs on the harmonic spectrum of the arterial pulse," *Amer. J. Clin. Med.*, **28**, No. 2, 279–289 (2000).
6. W. K. Wang, T. L. Hsu, and Y. Y. Wang, "Liu-wei-di-huang: a study by pulse analysis," *Amer. J. Clin. Med.*, **26**, No. 1, 73–82 (1998).
7. Y. Y. L. Wang, W. C. Lia, H. Hsiu, M.-Y. Jan, and W. K. Wang, "Effect of length on the fundamental resonance frequency of arterial models having radial dilatation," *IEEE Trans. Biomed. Eng.*, **47**, No. 3, 313–318 (2000).
8. M. G. Taylor, "The input impedance of an assembly of randomly branching elastic tubes," *Biophys. J.*, **6**, No. 1, 29–51 (1966).
9. D. J. Brown, "Input impedance and reflection coefficient in fractal-like models of asymmetrically branching compliant tubes," *IEEE Trans. Biomed. Eng.*, **43**, No. 7, 715–722 (1996).

10. M. Zamir, "Mechanics of blood supply to the heart: wave reflection effects in a right coronary artery," *Proc. Roy. Soc. London, Ser. B*, **265**, No. 1394, 439–444 (1998).
11. W. R. Milnor, *Hemodynamics*, Williams and Wilkins, Baltimore, etc. (1989).
12. I. N. Moiseeva and S. A. Regirer, "Certain characteristics of the pulse wave reflection in arteries," *Izv. Ros. Akad. Nauk, Mekh. Zhidk. Gaza*, No. 4, 134–139 (1993).
13. P. J. Reuderink, H. W. Hoogstraten, P. Sipkema, P. Hillen, and N. Westerhof, "Linear and nonlinear one-dimensional models of pulse wave transmission at high Womersley numbers," *J. Biomech.*, **22**, No. 8/9, 819–827 (1989).
14. W. Huang, R. T. Yen, M. McLaurine, and G. Bledsoe, "Morphometry of the human pulmonary vasculature," *J. Appl. Physiol.*, **81**, No. 5, 2123–2133 (1996).
15. D. Luzsa, *X-Ray Anatomy of the Vascular System* [in Russian], Acad. Kiado, Budapest (1973).
16. W. K. Wang, T. L. Hsu, Y. Chiang, and Y. Y. Wang, "The prandial effect of the pulse spectrum," *Amer. J. Clin. Med.*, **24**, No. 1, 93–98 (1996).

E-mail: knn@hall.nord.net.ua